frontiers | Frontiers in Marine Science

TYPE Original Research
PUBLISHED 12 March 2024
DOI 10.3389/fmars.2024.1348450

OPEN ACCESS

EDITED BY
Wenli Zhong,
Ocean University of China, China

REVIEWED BY
Matthew Buckley Alkire,
University of Washington, United States
Benjamin Rabe,
Alfred Wegener Institute Helmholtz Centre for Polar and Marine Research (AWI), Germany

*CORRESPONDENCE
Alexander Osadchiev
osadchiev@ocean.ru

RECEIVED 02 December 2023
ACCEPTED 29 February 2024
PUBLISHED 12 March 2024

CITATION
Osadchiev A, Kuskova E and Ivanov V (2024) The roles of river discharge and sea ice melting in formation of freshened surface layers in the Kara, Laptev, and East Siberian seas.
Front. Mar. Sci. 11:1348450.
doi: 10.3389/fmars.2024.1348450

The roles of river discharge and sea ice melting in formation of freshened surface layers in the Kara, Laptev, and East Siberian seas

Alexander Osadchiev[1,2,3]*, Ekaterina Kuskova[4] and Vladimir Ivanov[4,5]

[1]Shirshov Institute of Oceanology, Russian Academy of Sciences, Moscow, Russia, [2]Moscow Institute of Physics and Technology, Dolgoprudny, Russia, [3]Institute of Geology of Ore Deposits, Petrography, Mineralogy and Geochemistry, Russian Academy of Sciences, Moscow, Russia, [4]Lomonosov Moscow State University, Moscow, Russia, [5]Arctic and Antarctic Research Institute, Saint-Petersburg, Russia

Wide areas of the Siberian Arctic shelf are covered by freshened surface water layers, which are among the largest in the World Ocean. River discharge is the main freshwater source for formation of these layers; therefore, they are commonly referred to as river plumes (the Ob-Yenisei plume in the Kara Sea and the Lena plume in the Laptev and East Siberian seas). The contribution of sea ice meltwater (SIM) to the Ob-Yenisei and Lena plumes is pointed out to be small, albeit its actual volume remains unknown. In this study, we use a novel dataset of satellite-derived sea ice thickness in the Arctic Ocean during the melt period to quantify the annual volume of SIM, which was received by the Ob-Yenisei and Lena plumes during 2012–2020. We reveal that SIM is a significant source for the Lena plume providing, on average, 20% of total annual freshwater content. Moreover, the share of SIM in the Lena plume shows large inter-annual (14%–29%) variability, i.e., during certain years, SIM provides almost one-third of freshwater volume of the Lena plume. This variability is governed by inter-annual variability of ice thickness, as well as seasonal variability of sea ice melting conditions. Conversely, the contribution of SIM to the Ob-Yenisei plume is relatively low (8% on average), and its total annual share varies from 6% to 11% during the study period. This difference is mainly caused by significantly smaller area of the Ob-Yenisei plume as compared with the Lena plume. The forecasted earlier onset of ice melting in the Arctic Ocean in future decades due to climate change could decrease the contribution of SIM to the Ob-Yenisei plume, whereas its influence on the Lena plume remains unclear.

KEYWORDS

freshened surface layer, sea ice meltwater, river discharge, Ob-Yenisei plume, Lena plume, Arctic Ocean

1 Introduction

The freshwater cycle plays an important role in the Arctic Ocean due to its role in maintaining vertical salinity stratification (Aagaard et al., 1981; Nummelin et al., 2016). The well-developed halocline in the Arctic Ocean isolates the low salinity and cold surface layer (and also sea ice) from the warm and saline Atlantic water mass, which occupies intermediate depths (Polyakov et al., 2013; Carmack et al., 2015). The inflow, spreading, and transformation of different freshwater sources in the Arctic Ocean, namely, river runoff, net precipitation, sea ice meltwater (SIM), and Pacific waters, determine inhomogeneous salinity distribution in the surface layer (Aagaard and Carmack, 1989; Ekwurzel et al., 2001; Haine et al., 2015). Despite its key role in the formation of circulation and mixing patterns at the pan-Arctic scale and serious attention, which it received during the last decades, many aspects of hydrological cycle in the Arctic still remain poorly studied (Serreze et al., 2006; Carmack et al., 2016; Nummelin et al., 2016; Hall et al., 2023; Osadchiev et al., 2023b).

The freshwater sources in the Arctic mentioned above have different spatial localization, which strongly affects their fate. River runoff and Pacific water have distinct localized sources in river estuaries and the Bering Strait, respectively, located at the boundaries of the Arctic Ocean. As a result, they form consolidated and stable water masses (river plumes and Pacific halocline), which experience relatively slow mixing with ambient seawater (Carmack et al., 2015; Lin et al., 2021; MacKinnon et al., 2021; Osadchiev, 2021). In contrast, SIM and precipitation have non-localized sources, i.e., they provide dispersed freshwater fluxes at the surface throughout the Arctic Ocean. These freshwater sources do not form stable water masses but are mixed with ambient seawater as a result of wind and wave forcing (Skyllingstad et al., 2005; Vihma, 2014; Golovin and Ivanov, 2015; Alkire et al., 2017).

In this study, we focus on the interaction of two main freshwater sources on the Siberian shelf (Kara, Laptev, and East Siberian seas), namely, river runoff and SIM. This area receives very large river runoff (~2,500 km^3 annually), which forms two wide and distinct freshened surface layers in the Eurasian Arctic (Osadchiev et al., 2020a, b) (Figure 1). The first one is formed by the Ob and Yenisei rivers, which discharges inflow to the Kara Sea and coalesce into a joint Ob-Yenisei plume with an area of 200,000 km^2 to 250,000 km^2 (Osadchiev et al., 2021a). The second freshened area is formed by the Lena plume, which spreads over an area of 250,000 km^2 to 500,000 km^2 in the Laptev and East Siberian seas (Osadchiev et al., 2021b). Both river plumes have distinct seasonality in their formation and spreading. River flooding in late spring and early summer causes intense expansion of these plumes over the sea shelf. Later in late summer and autumn, river runoff drops by one order of magnitude. As a result, the active increase of plume areas is halted. Note that the Ob-Yenisei plume has very small inter-annual variability of the shape and position during the considered seasons (Osadchiev et al., 2021a) The Lena plume, in contrast, during different years could be either pressed toward the Siberian shore by prevailing northern and western winds with an area of ~250,000 km^2 or expanded northward by prevailing southern and eastern winds with an area of ~500,000 km^2 (Dmitrenko et al., 2005). This difference is caused by formation of the Lena plume by discharge from multiple shallow channels of the Lena Delta, which results in small depths and large stratification of the Lena plume and its quick response to wind forcing, as compared to the deeper and less stratified Ob-Yenisei plume, which is formed by two large and deep estuarine rivers (Osadchiev et al., 2021b).

SIM is another important freshwater source on the Siberian shelf. During the past decades of intensified summer retreat of sea ice in the Arctic Ocean, up to 2,000,000 km^2 to 2,500,000 km^2 of sea ice (1.5- to 2-m thick) melts during the warm season in the Kara, Laptev, and East Siberian seas (Wassmann et al., 2020; Sumata et al., 2023). As a result, ice melting provides up to 2,400 km^3 to 2,900 km^3 of freshwater annually, which is similar to annual river runoff. This huge volume of SIM is steadily delivered to the surface layer, but the intensity, duration, and exact dates of this flux demonstrate significant spatial inhomogeneity and inter-annual variability (Skyllingstad et al., 2005; Golovin and Ivanov, 2015). In

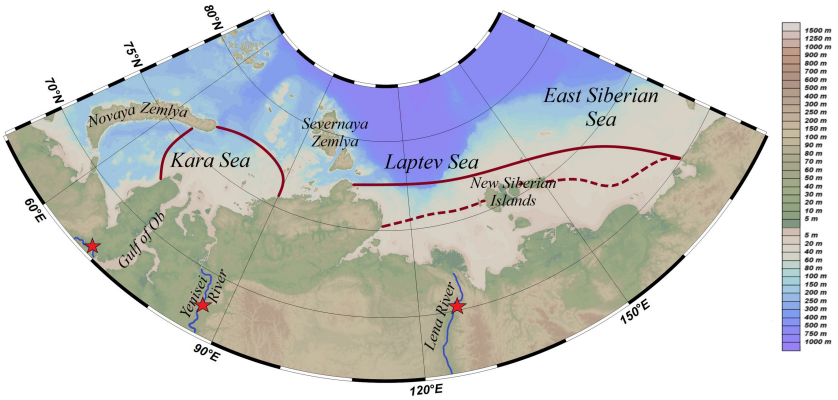

FIGURE 1
Bathymetry of the study area and the location of the Ob-Yenisei and Lena plumes during their maximal spreading in September. Red stars indicate location of gauge stations at the Ob, Yenisei, and Lena rivers. Note that the location of the outer border of the Lena plume was prescribed in two variants for predominant northern/eastern (solid line) and southern/western (dashed line) wind forcing conditions.

particular, the day when the Kara Sea becomes almost ice-free (which happens every year after 2007) and sea ice remains only at the northeastern periphery of the sea varies from the beginning of August (Figure 2A) to the middle of September (Figure 2B) (Duan et al., 2019; Osadchiev et al., 2021a). The sea ice coverage by the end of the melt period in the middle of September in the Laptev and East Siberian seas varies from 0 km^2 (during years when all sea ice melts) (Figure 2C) to 400,000 km^2 (during cold years with slow ice melting) (Figure 2D) (Liang and Su, 2021; Osadchiev et al., 2021b).

As was stated above, the Ob-Yenisei and Lena plumes are formed from localized freshwater sources, which provide their stability and relatively slow mixing with ambient saline seawater. Conversely, SIM is non-localized freshwater source. Once SIM is steadily received by the sea surface layer, it reduces surface salinity. This salinity anomaly steadily decreases due to mixing with subjacent seawater (Skyllingstad et al., 2005; Golovin and Ivanov, 2015; Dewey et al., 2017; Supply et al., 2022). Multiple *in situ* measurements have demonstrated that local salinity of the surface layer in the Kara, Laptev, and East Siberian seas (outside river plumes) several weeks after sea ice melt had ended was equal to 28–32, which is the typical salinity over these areas (Pavlov and Pfirman, 1995; Harms and Karcher, 1999; Zatsepin et al., 2010; Zavialov et al., 2015). Note that we define salinity according to EOS-80 (Fofonoff and Millard, 1983), hereafter simply referred to as "salinity".

Surface salinities in large river plumes in July and August are 15–20, which is much less than salinities in seawater freshened by SIM flux. Therefore, if a river plume is spreading over the seawater, freshened by SIM, then salinity difference between the river plume and seawater still remains very large and the plume is spreading above the seawater maintaining distinct vertical salinity gradient (Figure 3A). As a result, SIM remains below the river plume and limitedly contribute to its volume. Generally, certain mixing occurs between the advancing plume and seawater freshened by sea ice. However, assessments of this mixing for the Ob-Yenisei plume based on *in situ* data demonstrate that it is substantially lower than mixing within the plume (Osadchiev et al., 2021a) As a result, we assume the entrainment of SIM from seawater to the river plumes to be small enough and neglect it in our idealized model. A different situation occurs, when SIM is received by a river plume, i.e., ice melting occurs in the area, which is already occupied by a plume. In this case, freshwater flux from sea ice melting is discharged to a plume and is admixed to the plume water. Therefore, freshwater volume received from SIM remains within the plume and contributes to plume volume initially formed by river runoff (Figure 3B).

In previous studies of large river plumes in the Arctic Ocean, contribution of SIM was pointed out to be small or negligible. Evaluation of SIM share in the total freshwater content in the Ob-Yenisei and Lena plumes was based on analysis of nutrient concentration (Stunzhas, 1995; Makkaveev et al., 2010), stable isotopes (δD, $\delta^{18}O$) (Bauch et al., 2011; 2013; Dubinina et al., 2017a; b; Dubinina et al., 2019), and other geochemical tracers (Guay and Falkner, 1998; Jones et al., 1998; Ekwurzel et al., 2001; Yamamoto-Kawai et al., 2008; Paffrath et al., 2021). These previous studies provided the baseline for our understanding of the roles of river discharge, sea ice melting, ice formation, and brine release in formation of water masses in the study areas. In particular, they demonstrated that net ice formation at the Great Siberian Polynya during cold season dominates over ice melting during warm season due to intense ice export toward the central part of the Arctic Ocean by the Transpolar Drift (Bauch et al., 2011; 2013).

In this study, we evaluate freshwater volume of SIM, which is received by the Ob-Yenisei and Lena plumes and compare it with the freshwater volume provided by the river runoff. For this purpose, we use recently developed satellite-derived data on sea ice thickness, which covers the whole year including melting period from May to September (Landy et al., 2022). This dataset was made

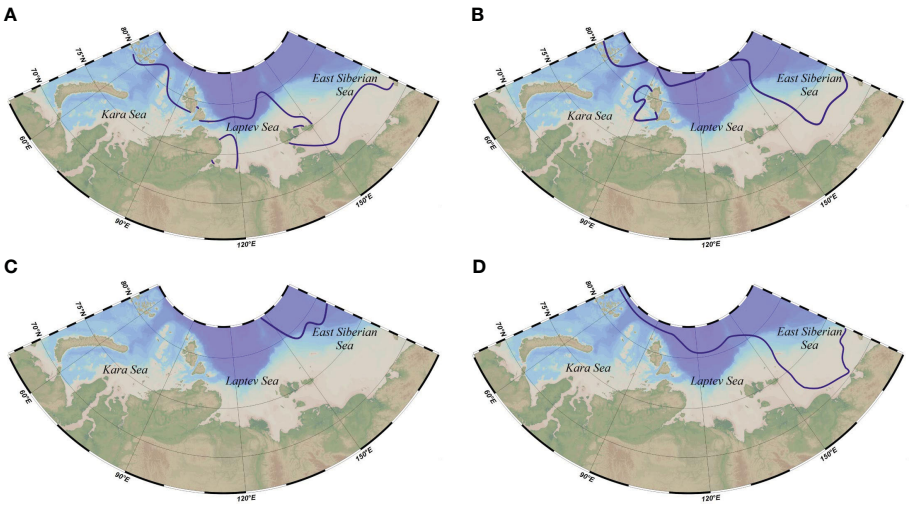

FIGURE 2
Examples of **(A)** early (4 August 2015) and **(B)** late (16 September 2014) ice-free conditions in the Kara Sea. Examples of **(C)** small (15 September 2020) and **(D)** large (15 September 2018) sea ice area by the end of melt season in the Laptev and East Siberian seas. Blue lines indicate location of the ice edge defined by the 15% of sea ice concentration.

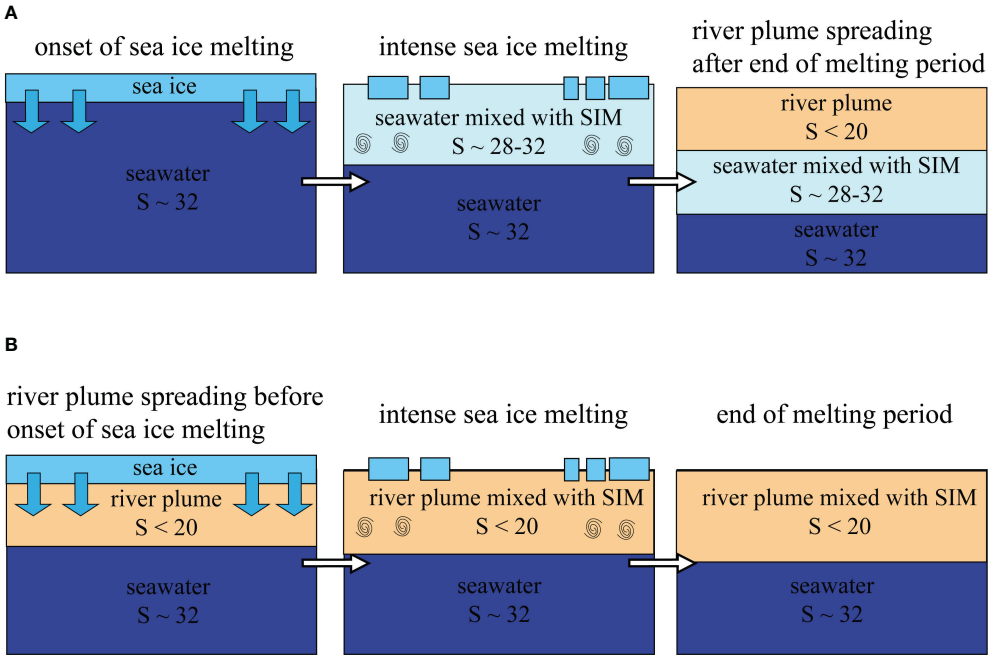

FIGURE 3
Schematic of SIM flux to **(A)** saline seawater and **(B)** river plume.

using machine learning and includes snow layer above the sea ice. Note that previously available data on sea ice thickness did not provide reliable information during melting period due to bias caused by presence of melt ponds on sea ice (Dawson et al., 2022). Usage of this dataset provides opportunity for direct calculations of SIM fluxes in the Arctic Ocean with spatial resolution of 80 km and temporal resolution of 2 weeks. We used these data to calculate the SIM fluxes to the expanding Ob-Yenisei and Lena plumes during May to September in 2012–2020. This volume was compared with river runoff data obtained from daily gauge measurements at the Ob, Yenisei, and Lena rivers. Note that our current study focuses on the specific ice melting process (only during warm season) and its influence on the surface layer, i.e., until the depths of 10 m to 20 m, which is occupied by river plumes, whereas previous studies mentioned above considered surface-to-bottom water column. In addition, our study deals with relatively high spatial and temporal resolution, whereas the previous studies generally considered net impact of river discharge, ice formation, and ice melting on the annual and inter-annual time scales.

This paper is organized as follows. In Section 2, we provide general information about sea ice thickness and river discharge data used in this study, as well as the methodology of calculating the flux of SIM to the Ob-Yenisei and Lena plumes during the warm season. Evaluation of shares of SIM and river runoff in the Ob-Yenisei and Lena plumes calculated every 2 weeks during May to September in 2012–2020 is described and compared in Section 3. Section 4 addresses seasonal and inter-annual variability of freshwater fluxes associated with river runoff and SIM, as well as discusses differences of SIM fluxes to the Ob-Yenisei and Lena plumes. The conclusions are given in Section 5.

2 Data and methods

Fluxes of SIM in the study area were calculated using maps of sea ice concentration derived from AMSR2 satellite data with spatial resolution of 6.25 km and temporal resolution of 1 day (Spreen et al., 2008) and sea ice thickness derived from Cryosat-2 satellite data with spatial resolution of 80 km and temporal resolution of 2 weeks (Landy et al., 2022) (Figure 4). The accuracy of these data validated against *in situ* measurements of sea ice thickness is estimated as 10 cm to 30 cm (Landy et al., 2022). Note that sea ice thickness maps cover the whole year including melting period from May to September in 2012–2020. Cumulative volume of freshwater flux from SIM during every 2 weeks at the 80-km grid points was calculated using the following equation $Q_{SIM} = \Delta V \cdot A_S \cdot A_V / S$, where $V = C_{ice} \cdot T_{ice}$ is the sea ice volume at the grid point equal to the product of sea ice concentration C_{ice} (reprojected to 80-km grid) and sea ice thickness T_{ice}, $A_S = 0.8$ is the coefficient to normalize meltwater salinity (prescribed equal to a salinity of 6) to fresh water (salinity of 0), $A_V = 0.9$ is the coefficient to normalize ice volume to meltwater volume, and $S = 640$ km^2 is the area of a grid cell. The accuracy of satellite sea ice concentration is estimated as 0.15 (Spreen et al., 2008). Natural variability of the applied values of A_S and A_V is equal to 0.1 for both parameters (Timco and Frederking, 1996).

Total freshwater flux from SIM to the Ob-Yenisei and Lena plume was calculated every 2 weeks in the following way. First, we determined location of the outer borders of the Ob-Yenisei and Lena plumes every 2 weeks in May to September. For both river plumes, location of borders was determined according to previously published *in situ* measurements of surface salinity data in the Kara,

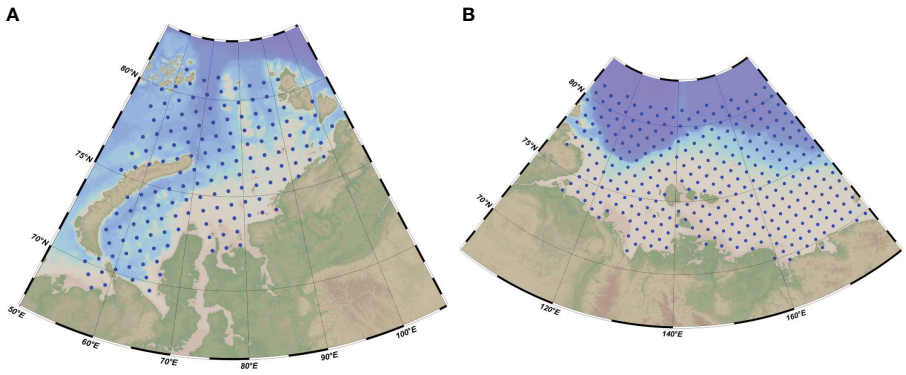

FIGURE 4
Grid points for calculation of SIM flux **(A)** in the Kara Sea and **(B)** in the Laptev and East Siberian seas.

Laptev, and East Siberian seas (Janout et al., 2020; Osadchiev et al., 2020b; Osadchiev et al., 2021a; b; Ashik, 2021; Spivak et al., 2021; Osadchiev et al., 2023a; Pipko et al., 2022; Xie et al., 2023) and climatology maps from the World Ocean database (2018) (Boyer et al., 2018). Location of the outer border of the Ob-Yenisei plume was prescribed the same for all considered years due to small inter-annual variability of position of this plume. Location of the outer border of the Lena plume was prescribed in two variants for predominant northern/eastern and southern/western wind forcing conditions, which result in southward (toward the Siberian coast) and northward (toward the shelf break) advection of the plume, respectively. The first variant corresponded to conditions in 2013–2015 and 2019–2020, whereas the second variant corresponded to conditions in 2012 and 2016–2018 (Janout et al., 2020; Osadchiev et al., 2021b). Finally, at every 2 week step, total freshwater flux from SIM to the Ob-Yenisei and Lena plume was calculated by summarizing fluxes around all grid cells located within the borders of these plumes during the respective time period. Freshwater flux from SIM located outside the plume borders was considered as the flux to the saline seawater. Due to the large size of a grid cell (80 km), advection of sea ice between the cells during the 2 week periods was neglected. Similar, we neglect advection of sea ice inside and outside the study areas in the Kara Sea (Figure 4A) and the Laptev and East Siberian seas (Figure 4B), because their prescribed limits are located far from the Ob-Yenisei and Lena plume borders, respectively.

River discharge data were obtained on a daily basis from the most downstream gauge stations at the Ob, Yenisei, and Lena rivers, namely, Salekhard, Igarka, and Kyusyur, respectively (red stars in Figure 1). In order to reproduce the role of smaller rivers (the Pyasina, Taz, Pur, and Nadym rivers, which are not covered by gauge measurements) in formation of the Ob-Yenisei plume, the cumulative daily discharge of the Ob and Yenisei rivers was multiplied by 1.2 according to ratio between the total annual discharge of the Ob and Yenisei rivers and smaller rivers (Gordeev et al., 1996). Similarly, daily discharge of the Lena River was multiplied by 1.55 in order to reproduce the role of the Kolyma, Indigirka, Olenyok, and Yana rivers in formation of the Lena plume.

3 Results

The calculated annual freshwater fluxes from river discharge and SIM to the Ob-Yenisei and Lena plumes during 2012–2020 and the uncertainties of fluxes (Tank et al., 2023) are presented in Figure 5. At the first approximation, river discharge plays much greater role than SIM in the formation of the Ob-Yenisei plume in the Kara Sea. The total annual contribution of SIM to the Ob-Yenisei plume varies between 57 km^3 and 93 km^3 (with an average of 80 km^3) (solid blue line in Figure 5). Total annual river discharge to the Ob-Yenisei plume is one order of magnitude greater, namely, 631 km^3 to 1,038 km^3 (with an average of 907 km^3) (solid red line in Figure 5). As a result, the share of SIM in the freshwater budget of the Ob-Yenisei plume varies from 6% to 11% among different years with an average value of 8% (Figure 6A). Total annual contribution of SIM to the Lena plume varies between 132 km^3 and 302 km^3 (with an average of 193 km^3), which is two to three times greater than in the Kara Sea (dashed blue line in Figure 5). This difference is caused by significantly greater area of the Lena plume as compared with the Ob-Yenisei plume. Total annual river discharge to the Lena plume is 537 km^3 to 871 km^3 (with an average of 782 km^3), which is slightly smaller than that to the Ob-Yenisei plume (dashed red line in Figure 5). Therefore, the share of SIM in the freshwater budget of the Lena plume varies from 14% to 29% among different years with average value of 20% (Figure 6B), which is ~2.5 times greater than in the Ob-Yenisei plume. As a result, in the Laptev and East Siberian seas, river discharge also dominates in the income freshwater budget of the Lena plume; however, the role of SIM is more significant as compared to the Ob-Yenisei plume in the Kara Sea. In particular, in 2017 and 2019, SIM provided more than one quarter of total freshwater volume in the Lena plume.

Biweekly distributions of freshwater fluxes from SIM to the Ob-Yenisei and Lena plumes during ice melting season in 2012–2020 are presented in Figure 7. They demonstrate significant seasonal and inter-annual variability of SIM fluxes. In the Kara Sea, SIM fluxes demonstrate one distinct peak which occurs from the end of May until the end of June (Figure 7A). The annual peak varies between the different years from 25 km^3 to 64 km^3. SIM flux in August and September decreases to zero, because, by early August,

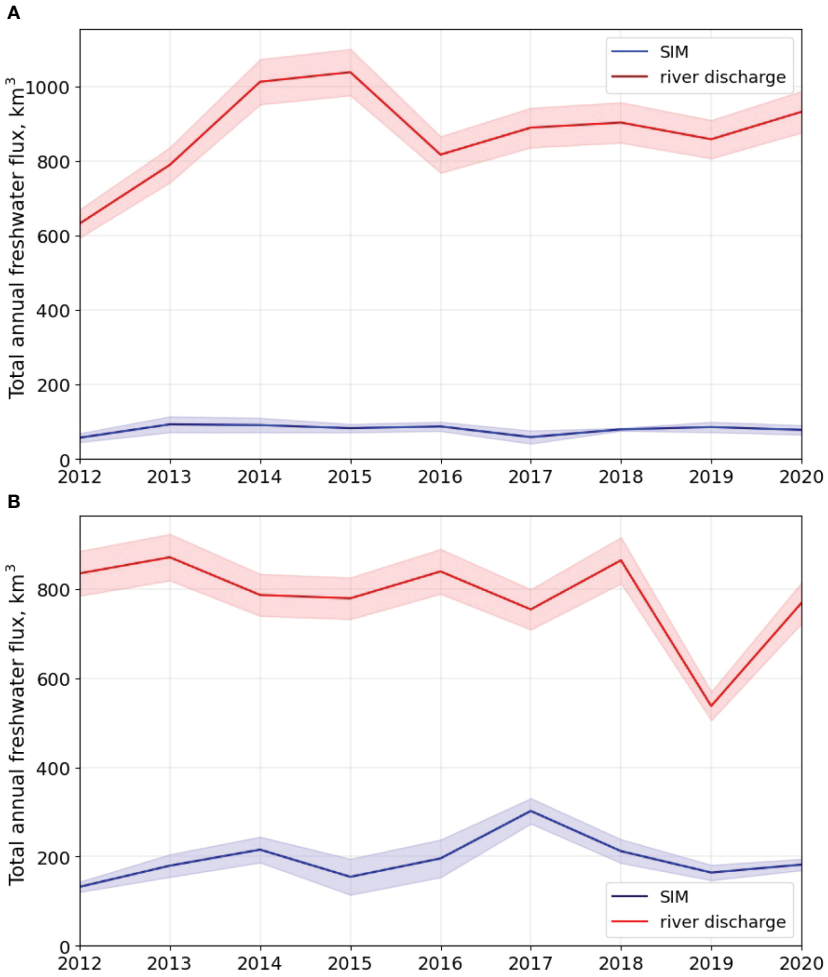

FIGURE 5
Total annual freshwater fluxes from river discharge (red lines) and SIM (blue lines) to the Ob-Yenisei plume **(A)** and the Lena plume **(B)** during 2012–2020. Shaded areas indicate the uncertainties of fluxes.

the spreading area of the Ob-Yenisei plume in the Kara Sea becomes ice-free.

In the Laptev Sea, two distinct peaks of SIM fluxes are observed (Figure 7B). The first peak of SIM flux (38 km^3 to 109 km^3) is observed in June every year (except 2012) and is associated with an increase of the Lena plume area due to the start of the flooding period. The second peak of SIM flux is registered during certain years in late July and early August and is associated with intensified summer melting of sea ice remaining in the southern parts of the Laptev and East Siberian seas. Maximal biweekly SIM flux during this period varies from 23 km^3 to 49 km^3. Then, SIM flux significantly decreases; however, during certain years, sea ice melting in the Laptev and East Siberian seas continues until late September, i.e., the end of the warm season.

Large seasonal and inter-annual variability of SIM and riverine freshwater fluxes during the warm period results in variability of their relative shares in the river plumes. Once intense sea ice melting starts before the peak river discharge, the share of SIM could become similar to the share of the river discharge during late spring. This situation is common for the Lena plume and was observed in 2013, 2017, and 2019 in May when the share of SIM in total freshwater content in the Lena plume was up to 15%–25%. In contrast, in the Kara Sea, this situation does not occur due to earlier start of the flooding period (Figure 8).

As a result, average biweekly freshwater flux from SIM to the Ob-Yenisei plume is one order of magnitude less than freshwater flux from river discharge due to overlap of periods of peak river discharge and the most intense sea ice melting in the Kara Sea (solid lines in Figure 9). Average biweekly share of SIM in total freshwater volume in the Ob-Yenisei plume increases from 1% in spring to 11% in summer and then decreases to 8% in autumn (Figure 10). Conversely, in the Laptev and East Siberian seas, freshwater flux from SIM is comparable with that from river discharge: first, during late spring due to smaller river discharge at spring drought conditions and, second, during late summer due to longer ice melting period (dashed lines in Figure 9). Average biweekly share of SIM in the total freshwater volume in the Lena plume is 2% at the onset of the melting season in May, followed by an increase to 23% in summer and decrease to 20% in autumn (Figure 10). Note that averaging during nine considered years of SIM fluxes (Figure 9) and SIM shares (Figure 10) removed the peak of SIM share for the Lena plume at the beginning of ice melting period, which occurred only

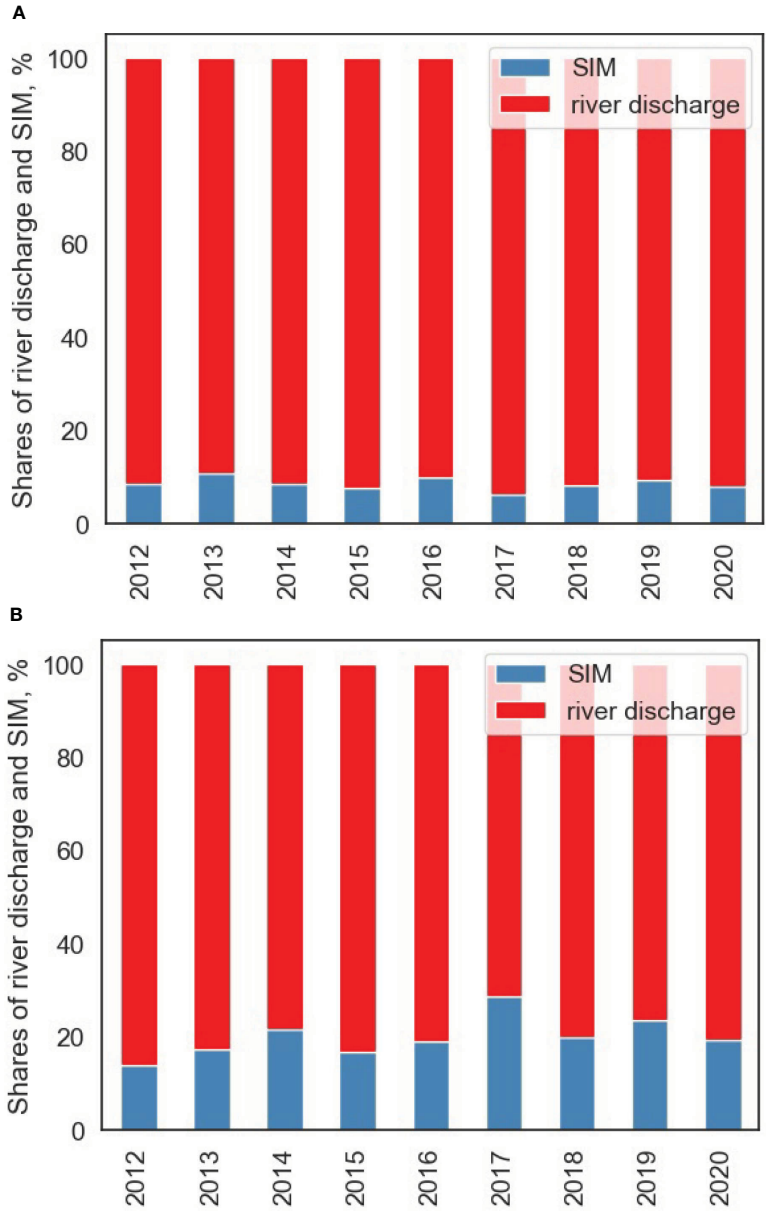

FIGURE 6
Shares of river discharge (red) and SIM (blue) in total freshwater volume in **(A)** the Ob-Yenisei plume and **(B)** the Lena plume during 2012–2020.

during 2013, 2017, and 2019 (Figure 8), and smoothened the double peak of SIM flux for the Lena plume in June to July (Figure 7B).

4 Discussion

Large seasonal and inter-annual variability of SIM flux to the Ob-Yenisei and Lena plumes described in the previous section is governed by variability of sea ice conditions. Sea ice melting at the certain sea area contributes to a river plume only if the plume has already spread below the sea ice in this area (Figure 3B). Once sea ice melting occurred outside a river plume, it would not be received by the plume even if the plume will later spread in this area (Figure 3A). This feature occurs due to much smaller salinities in the large Arctic plumes as compared to saline seawater freshened by SIM. In order to understand the relationship between sea ice conditions and SIM fluxes to the Ob-Yenisei and Lena plumes, we analyze examples of years with small and large SIM flux to the Ob-Yenisei plume (Figure 11) and to the Lena plume (Figure 12).

Figure 11 demonstrates that total annual SIM contribution to the Ob-Yenisei plume is governed by coalescence of intense sea ice melting and intense expansion of the plume. Once all sea ice melted early before the Ob-Yenisei plume spread over wide area in the central part of the Kara Sea, the SIM flux to the plume is low. In particular, this situation was observed in 2012 when the lowest contribution of SIM to the Ob-Yenisei plume was registered among the considered years (Figure 5). Due to warm atmospheric conditions during this year, the central part of the Kara Sea

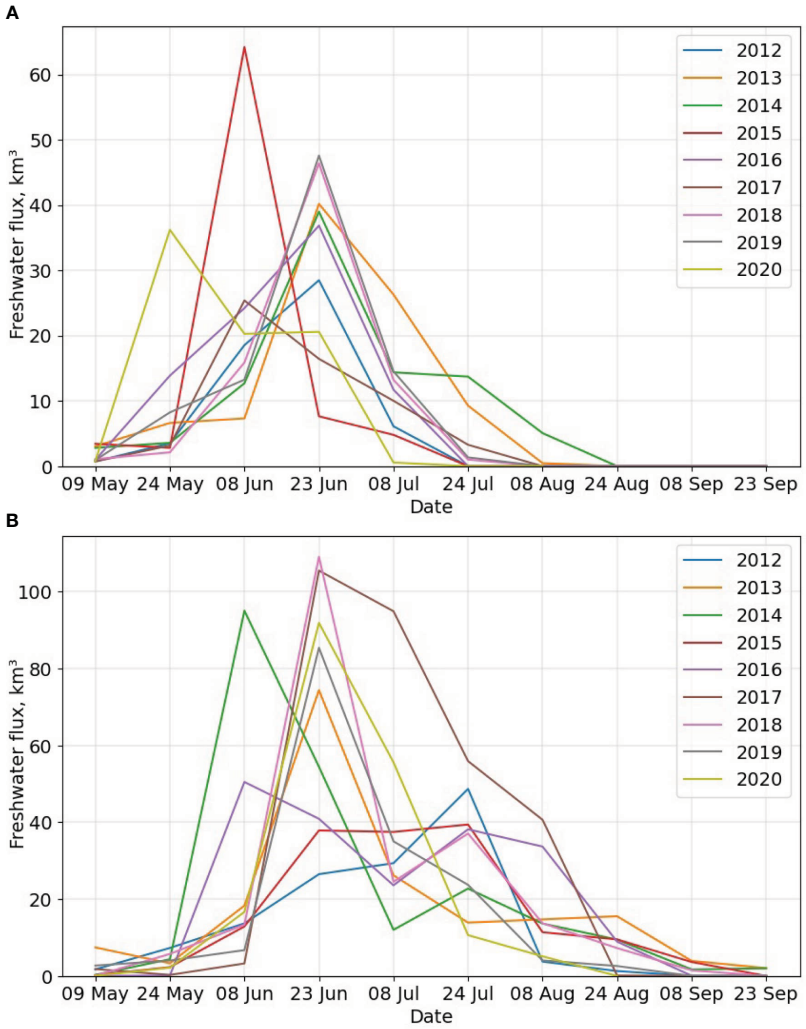

FIGURE 7
Biweekly freshwater flux from SIM to **(A)** the Ob-Yenisei plume and **(B)** the Lena plume from 9 May to 23 September during 2012–2020.

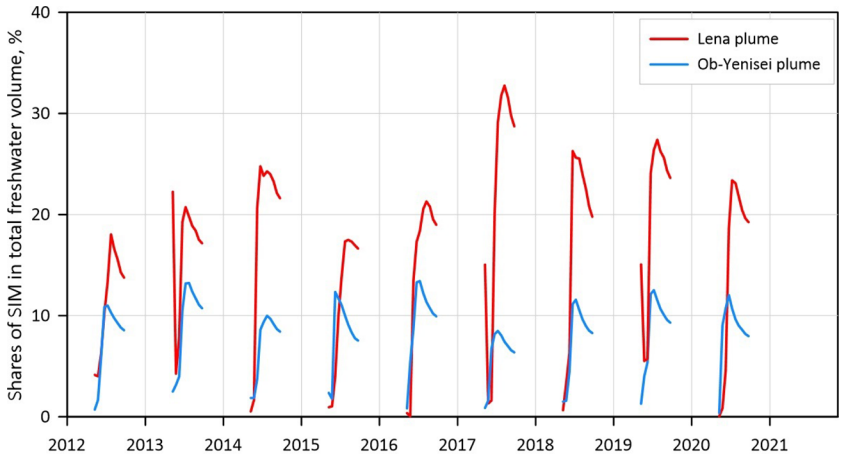

FIGURE 8
Biweekly shares of SIM in total freshwater volume in the Ob-Yenisei plume (blue lines) and the Lena plume (red lines) from 9 May to 23 September during 2012–2020.

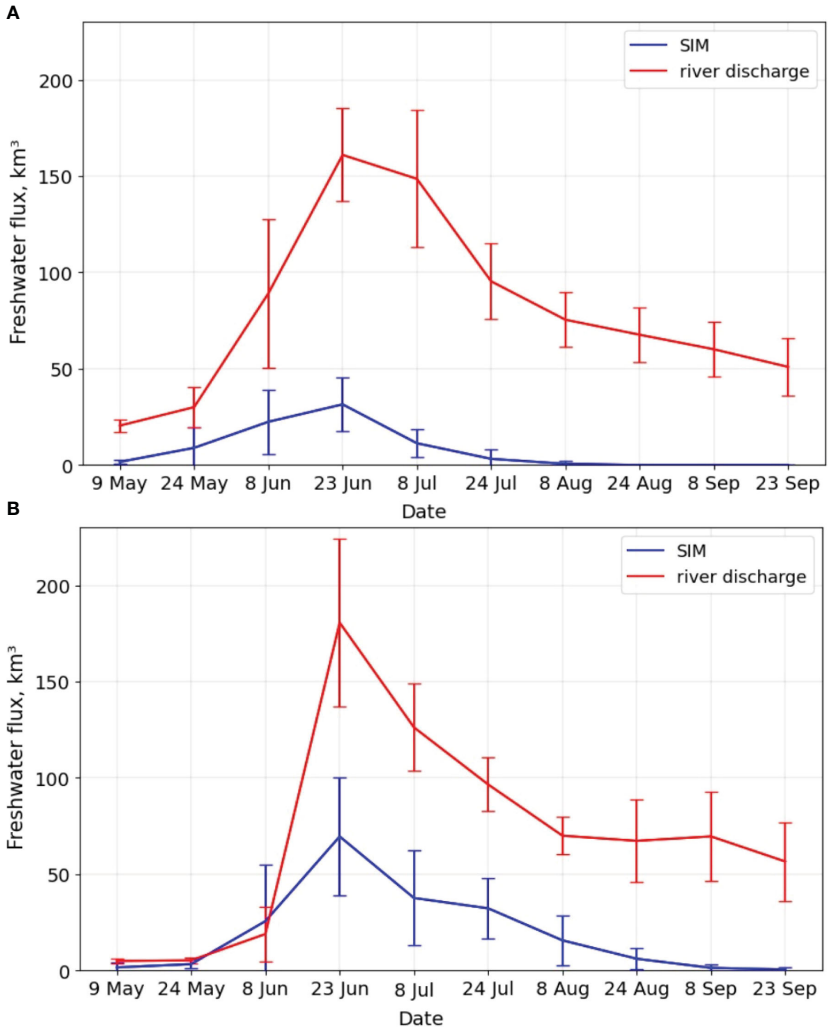

FIGURE 9
Average biweekly freshwater flux from river discharge (red lines) and SIM (blue lines) to Ob-Yenisei plume **(A)** and the Lena plume **(B)** from 9 May to 23 September. The whiskers show standard deviations of the biweekly freshwater fluxes.

became almost free of ice by the beginning of July, which is very early for this area (Figure 11A). This resulted in small SIM flux to the Ob-Yenisei plume during peak flooding period in late June and the subsequent reduction of SIM flux to zero by late July (blue line in Figure 7A). The opposite situation of late sea ice melting in the central part of the Kara Sea was observed in 2013. During this year, ice remained in the central part of the Kara Sea until early August (Figure 11B), which resulted in high values of SIM flux to the plume during two months in June and July (orange line in Figure 7A) and the largest total share of SIM in freshwater content of the Ob-Yenisei plume (Figure 5).

As a result, early/late onset of intense sea ice melting in the central part of the Kara Sea, which is occupied by the Ob-Yenisei plume by late June and early July, preconditions low/high SIM flux to the Ob-Yenisei plume. Late onset of sea ice melting in the central part of the Kara Sea significantly reduces period of local ice melting, because every year the ice completely disappears in this part of the sea by mid-September. Sea ice could remain during the whole year in the Kara Sea only in its eastern part and only in certain years (e.g., 2014 and 2021). This part of the sea becomes partly occupied by the plume in August and September. Nevertheless, inter-annual variability of sea ice conditions in this area plays much smaller role in the contribution of SIM to the Ob-Yenisei plume due to, first, low intensity of this flux in August and September and, second, relatively small area of the plume in this part of the sea.

The most intense sea ice melting in the Laptev and East Siberian seas occurs in June and July and provides the largest SIM fluxes to the Lena plume during the warm season (Figure 7B). As a result, similar to the Kara Sea, early/late onset of sea ice melting in the southeastern part of the Laptev Sea and southwestern part of the East Siberian Sea, before active spreading of the Lena plume decreases/increases SIM flux to the plume. In particular, this situation was observed in 2012 (Figure 5B) when, similarly to the Kara Sea, the southern parts of the Laptev and East Siberian seas became almost free of ice in the beginning of August, which is very early for this area (Figure 12A). This resulted in moderate values of SIM flux during relatively short period from late June until late July (blue line in Figure 7B). The opposite situation of late onset of

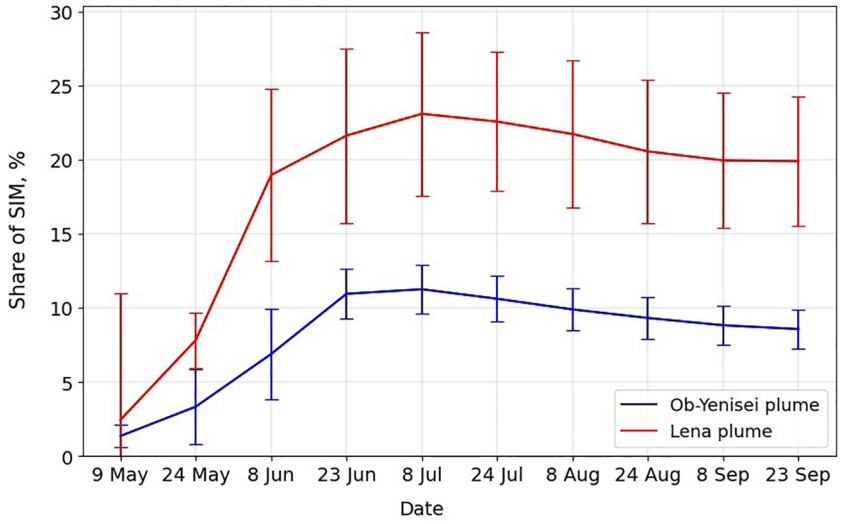

FIGURE 10
Average biweekly shares of SIM in total freshwater volume in the Ob-Yenisei plume (blue line) and the Lena plume (red line) during 2012–2020. The whiskers show standard deviations of the biweekly shares of SIM.

intense sea ice melting was observed in 2017 (Figure 12B) when ice melting provided large SIM flux to the Lena plume from early June until early August (brown line in Figure 7B).

Sea ice conditions in the Laptev and East Siberian seas by the end of the melting period in the middle of September also play an important role in inter-annual variability of SIM contribution to the Lena plume. In contrast to the Kara Sea, during certain years, the central parts of the Laptev and East Siberian seas could be covered by ice which results in SIM flux to the Lena plume in August and September. These freshwater fluxes are smaller than those observed in June and July but could provide up to 30 km^3 to 40 km^3 of freshwater volume to the Lena plume (e.g., in 2017 and 2018) (Figure 7B). Another important factor that affects SIM fluxes to the Lena plume is inter-annual variability of ice thickness in the southern parts of the Laptev and East Siberian seas (Figure 13). Ice melting at these areas provides SIM flux to the Lena plume in June and early July when it has relatively small area. In particular, small SIM flux to the Lena plume in June in 2012 was caused by relatively small ice thickness in the southern part of the Laptev Sea (1 m to 1.5 m) (Figure 13A), whereas large SIM flux in June in 2017 was provided by thick ice (1.5 m to 2 m) in the southeastern part of the Laptev Sea in vicinity of the Lena Delta (Figure 13B).

Finally, the small/large mode of the Lena plume that is governed by wind forcing conditions (Dmitrenko et al., 2005; Janout et al., 2020; Osadchiev et al., 2021b) plays a less significant role in inter-annual variability of contribution of SIM to the plume. Small and large SIM fluxes to the Lena plume were observed during both years with small plume area (2012 and 2017, respectively) and large plume area (2015 and 2014, respectively). This feature is caused by relatively low SIM flux from sea ice melting in the northern parts of the Laptev and East Siberian seas due to, first, short residence time of the plume in this area in late August and September and, second, already low intense sea ice melting during this period. This result contradicts the findings of Bauch et al. (2013), which associated large area of the Lena plume observed in 1994 and 2008 with intense sea ice melting as compared to small river plume area in 2007 and 2009. Nevertheless, our assessments of SIM contribution to the Lena plume equal to 132 km^3 to 302 km^3 in 2012–2020 are in good agreement with the related assessments based on analysis of stable isotopes equal to 109 km^3 and 158 km^3 in 1994 and 2008.

5 Conclusions

In this study, using novel satellite data of sea ice thickness in the Arctic Ocean (Landy et al., 2022), we calculated SIM fluxes in the Kara, Laptev, and East Siberian seas during warm season (9 May to 23 September) in 2012–2020 with spatial resolution of 80 km and temporal resolution of 2 weeks. Then, we evaluated freshwater volume, which was received from SIM by the Ob-Yenisei plume in the Kara Sea and by the Lena plume in the Laptev and East Siberian seas during the considered periods. We compared this volume with river runoff that forms the Ob-Yenisei and Lena plumes in order to evaluate the roles of river discharge and sea ice melting in formation of these plumes and understand seasonal and inter-annual variability of shares from both freshwater sources. The accuracy of the obtained results is limited by the accuracy of the satellite-derived sea ice thickness data, which was used in this study. Nevertheless, to the extent of our knowledge, they provide the first comprehensive assessment of the role of sea ice melting in formation of the freshened surface layers in the Kara, Laptev, and East Siberian seas.

We reveal that the contribution of SIM to the Ob-Yenisei plume is relatively low (8% on average) and its total annual share varies from 6% to 10% in 2012–2020. Maximal freshwater flux from SIM received by the Ob-Yenisei plume during the study period was registered in 2013 and was equal to 93 km^3. During the warm season, the average share of SIM in total freshwater volume in the

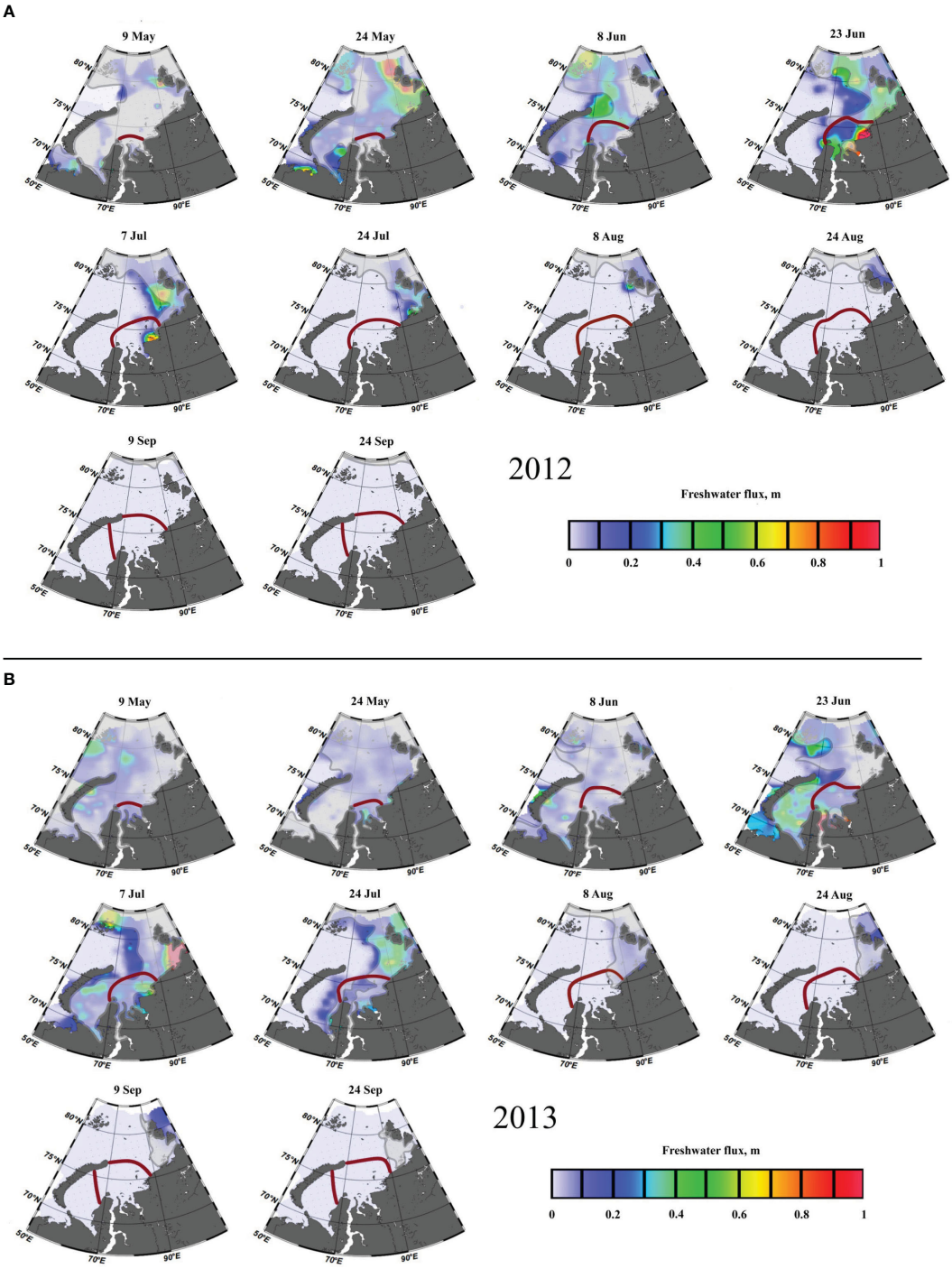

FIGURE 11
Distributions of biweekly freshwater flux from SIM to the Kara Sea from 9 May to 23 September in **(A)** 2012 and **(B)** 2013, illustrating conditions resulting in **(A)** small and **(B)** large SIM flux to the Ob-Yenisei plume. Red lines indicate location of the outer Ob-Yenisei plume border, and gray lines and gray shading indicate location of sea ice.

Ob-Yenisei plume increases from 1% in spring to 11% in summer and then decreases to 8% in autumn. This feature is caused by early ice melting in the Kara Sea, which occurs before the Ob-Yenisei plume becomes well-developed and occupies large area. As a result, the majority of SIM is mixed with saline seawater outside the plume and does not form stable freshened surface layer in the Kara Sea. The Ob-Yenisei plume is later spreading above the mixed seawater and SIM due to its significantly lower salinities.

The opposite situation is observed in the Laptev and East Siberian seas. SIM is a significant source for the Lena plume providing on average 20% of total annual freshwater content due to much greater spreading area of the Lena plume as compared with

10.3389/fmars.2024.1348450

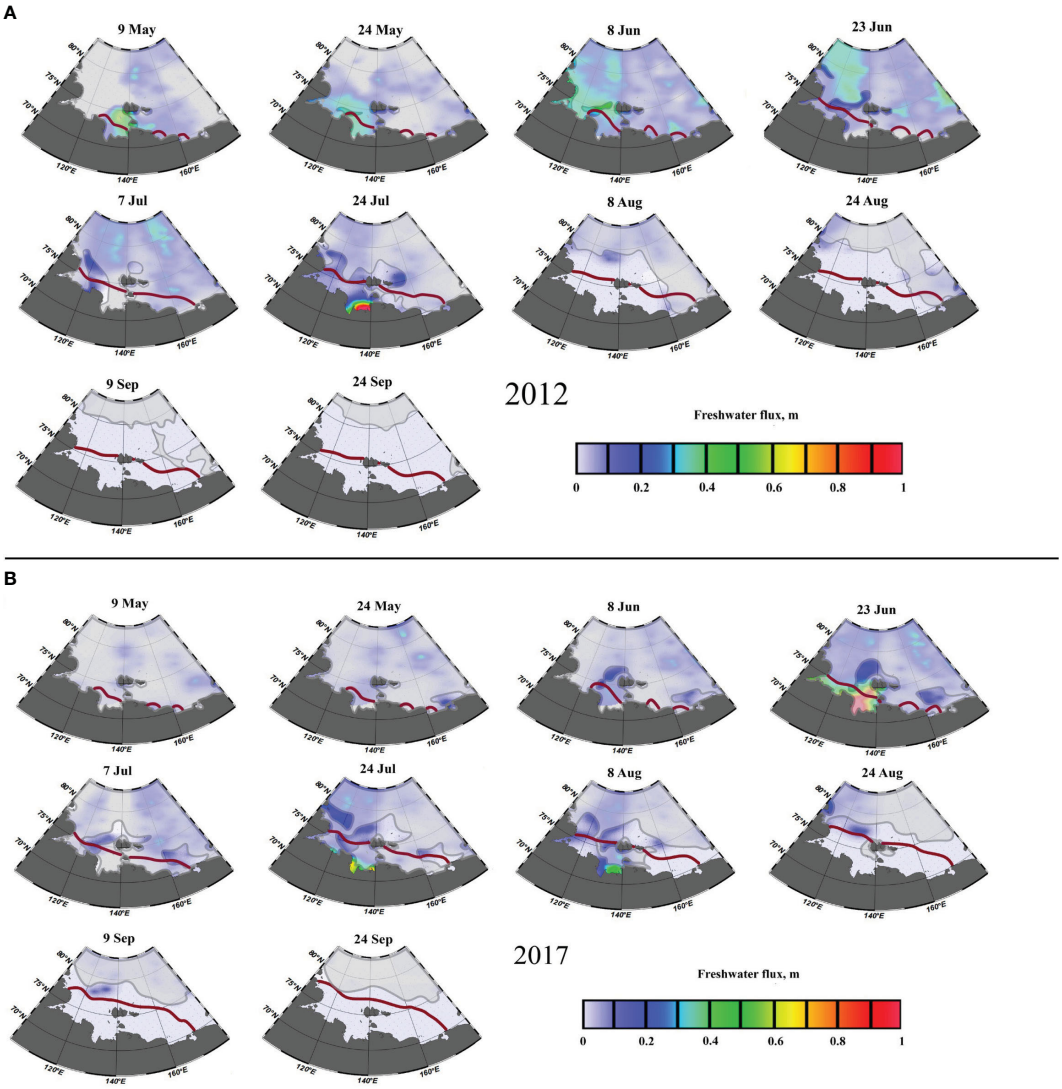

FIGURE 12
Distributions of biweekly freshwater flux from SIM to the Laptev and East Siberian seas from 9 May to 23 September in **(A)** 2012 and **(B)** 2017, illustrating conditions resulting in **(A)** small and **(B)** large SIM flux to the Lena plume. Red lines indicate location of the outer Lena plume border, and gray lines and gray shading indicate location of sea ice.

the Ob-Yenisei plume. Moreover, the share of SIM to the Lena plume shows large inter-annual (14%–29%) variability, i.e., during certain years SIM provides almost one-third of the freshwater volume of the Lena plume. In particular, in 2017, the freshwater volume received by the Lena plume from SIM was equal to 302 km^3. Inter-annual variability of SIM volume in the Lena plume is governed by inter-annual variability of the Lena plume spreading area, as well as seasonal variability of sea ice melting conditions. During the warm season, the average share of SIM in the total freshwater volume in the Lena plume increases from 2% in spring to 23% in summer and then decreases to 20% in autumn. The largest contribution of SIM to the Lena plume occurs during years when ice melting is late but intense. In this case, the main ice melting period starts after the initial freshet spreading of the Lena plume, i.e., when the plume already occupied large area in the sea, and, therefore, SIM produced at this area is captured by the plume. Another important condition is that ice melting is intense, and, despite late start, large volume of SIM is produced during the melt season and the Laptev and East Siberian shelves become ice-free by the middle of September.

Sea ice melts by the beginning of September at all spreading area of the Ob-Yenisei plume during every year. As a result, SIM flux to the Ob-Yenisei plume is controlled mainly by interposition of the onset of intense ice melting in the central part of the Kara Sea. The second important factor is the start of the intense expanding of the Ob-Yenisei plume caused by the beginning of the flooding period at the Ob and Yenisei rivers. Early/late onset of intense ice melting preconditions low/high contribution of SIM to the Ob-Yenisei plume. In summary, the main prediction of high total annual SIM flux to the Ob-Yenisei plume is the presence of large area covered by sea ice in the central part of the Kara Sea in late June and early July.

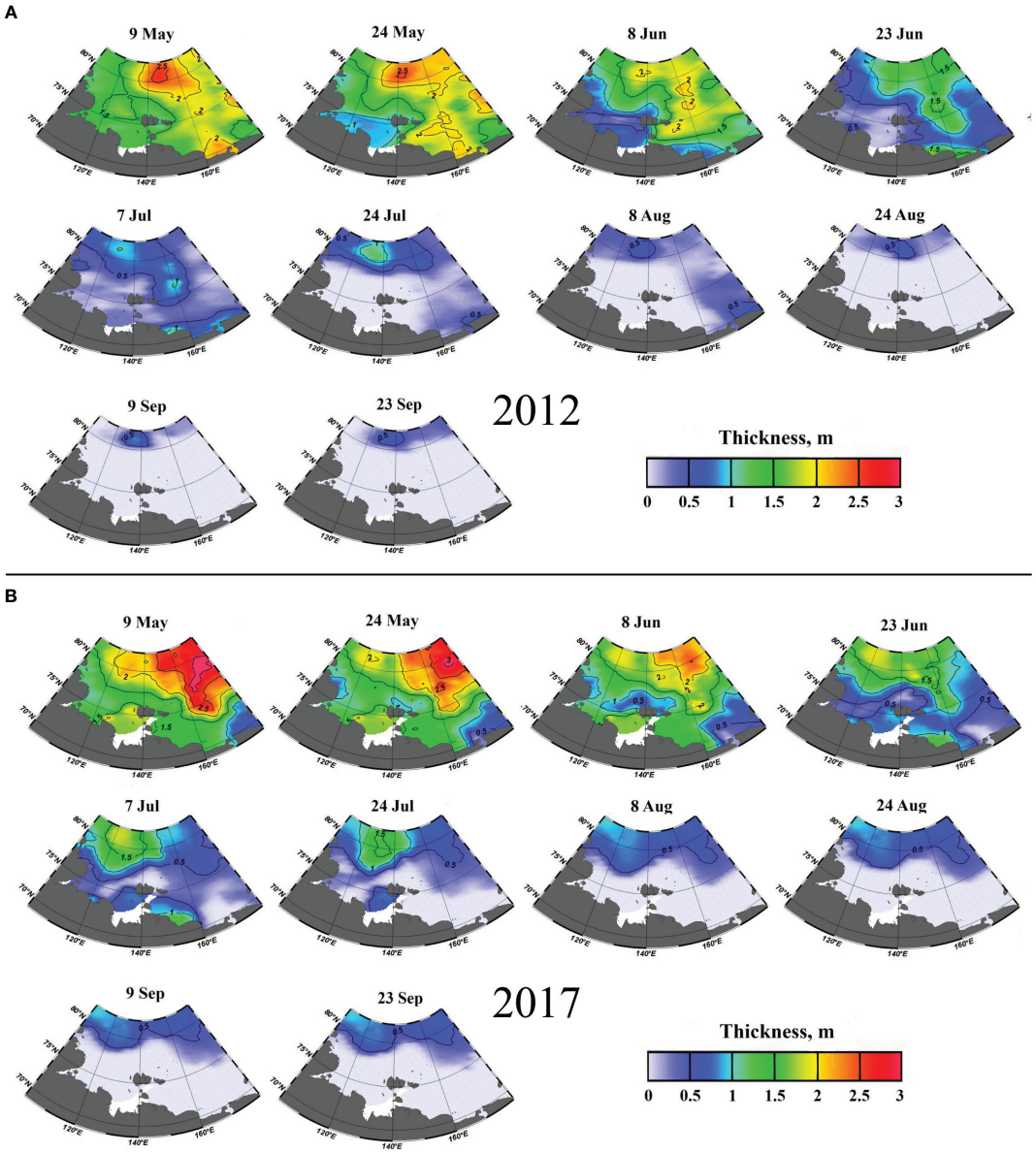

FIGURE 13
Sea ice thickness in the Laptev and East Siberian seas from 9 May to 23 September in **(A)** 2012 and **(B)** 2017.

Similar to the Ob-Yenisei plume, a large annual SIM flux to the Lena plume is provided by late onset of intense ice melting in the southeastern part of the Laptev Sea and the southwestern part of the East Siberian Sea, which are occupied by the Lena plume shortly after the beginning of the flooding period. However, sea ice conditions in the Laptev and East Siberian seas also play an important role in this process due to greater thickness of fast sea ice in the southeastern part of the Laptev Sea (Timofeeva and Sharatunova, 2021), which provide the main SIM flux before the Lena plume becomes well-developed. In addition, the presence of sea ice at the spreading area of the Lena plume during the whole warm season results in significant SIM fluxes to the Lena plume in August and September (which are off the peak ice melting season in June and July). In summary, the main prediction of the high total annual SIM flux to the Lena plume includes, first, the presence of large area covered by thick sea ice in the southeastern part of the Laptev Sea and the southwestern part of the East Siberian Sea in June and July and, second, the absence of sea ice in the central and southern part of these seas in the middle of September.

Spreading and transformation of freshened surface layer in the Arctic Ocean influence many local physical, biological, and geochemical processes including biological productivity (Demidov et al., 2014; Mosharov et al., 2018; Kopylov et al., 2023), carbon cycle (Pipko et al., 2022), and transport of pollutants (Pogojeva et al., 2021; Yakushev et al., 2021). This fact highlights the importance of study of large-scale freshwater cycle in the Arctic Ocean. Future changes in sea ice melting in the Arctic Ocean as a result of global warming could modify the roles of river discharge and sea ice melting in formation of the Ob-Yenisei and Lena plumes. Earlier onset of sea ice melting by several days in a decade, which is observed in the Kara, Laptev, and East Siberian seas (Stroeve and Notz, 2018), tends to reduce the volume of

SIM in the Ob-Yenisei plume due to relatively short ice melting season in the Kara Sea but increases this volume in the Lena plume, because, during most years, ice melting in the Laptev and East Siberian seas continues during the whole warm season. However, if ice conditions in the Laptev and East Siberian seas will change and these seas will become free (or almost free) of ice by the end of warm season in the middle of September (which is already the case for the Kara Sea), then earlier onset of sea ice melting would also tend to reduce the volume of SIM in the Lena plume.

The possible future increase of SIM contribution to the Lena plume would strongly affect the shelf–basin interaction along the Laptev and East Siberian seas (Anderson et al., 2010; 2017). The increase of area and volume of the Lena plume would strengthen stratification and reduce vertical mixing between the freshened surface layer and the halocline (Carmack et al., 2016). Moreover, this process has potential to intensify upwelling at the shelf break of the Laptev Sea in case of favorable local wind and sea ice conditions (Carmack and Chapman, 2003) and cause increase in biological productivity along the Arctic shelf break (Randelhoff and Sundfjord, 2018). An increase of river discharge to the Arctic Ocean and, in particular, the increase of annual runoff from the Yenisei and Lena rivers by several percent over decade (Feng et al., 2021) would reduce the average share of SIM in freshwater content of the Ob-Yenisei and Lena plumes. However, these trends are much less than the observed inter-annual variability of the river runoff and, therefore, they play a secondary role in the variability of share of SIM in freshwater content of the plumes as compared to sea ice conditions. Finally, it is important to forecast the start of the flooding period for the Ob, Yenisei, and Lena rivers, which could also become earlier due to climate change and affect the share of SIM in the Ob-Yenisei and Lena plumes.

Data availability statement

The original contributions presented in the study are included in the article/supplementary material. Further inquiries can be directed to the corresponding author.

Author contributions

AO: Writing – review & editing, Writing – original draft, Formal analysis, Conceptualization. EK: Writing – original draft, Visualization, Methodology, Formal analysis, Data curation. VI: Writing – review & editing, Methodology, Formal analysis.

Funding

The author(s) declare that financial support was received for the research, authorship, and/or publication of this article. This research was funded by the Ministry of Science and Higher Education of the Russian Federation, theme FMWE-2021-0001 (processing of satellite data); the Moscow Institute of Physics and Technology development program (Priority-2030) (processing of sea ice data); and the Russian Science Foundation, research projects 23-17-00087 (study of river plumes in the Arctic Ocean) and 23-17-00001 (study of sea ice meltwater in the Arctic Ocean).

Conflict of interest

The authors declare that the research was conducted in the absence of any commercial or financial relationships that could be construed as a potential conflict of interest.

Publisher's note

References

Aagaard, K., and Carmack, E. C. (1989). The role of sea ice and other fresh water in the Arctic circulation. *J. Geophys. Res. Oceans* 94, 14485–14498. doi: 10.1029/JC094iC10p14485

Aagaard, K., Coachman, L., and Carmack, E. (1981). On the halocline of the arctic ocean. *Deep Sea Res.* 28, 529–547. doi: 10.1016/0198-0149(81)90115-1

Alkire, M. B., Morison, J., Schweiger, A., Zhang, J., Steele, M., Peralta-Ferriz, C., et al. (2017). A meteoric water budget for the Arctic Ocean. *J. Geophys. Res. Oceans* 122, 10020–10041. doi: 10.1002/2017JC012807

Anderson, L. G., Björk, G., Holby, O., Jutterström, S., Mörth, C. M., O'Regan, M., et al. (2017). Shelf–basin interaction along the East Siberian Sea. *Ocean Sci.* 13, 349–363. doi: 10.5194/os-13-349-2017

Anderson, L. G., Tanhua, T., Björk, G., Hjalmarsson, S., Jones, E. P., Jutterström, S., et al. (2010). Arctic Ocean shelf–basin interaction: An active continental shelf CO2 pump and its impact on the degree of calcium carbonate solubility. *Deep-Sea Res. I: Oceanogr. Res.* 57, 869–879. doi: 10.1016/j.dsr.2010.03.012

Ashik, I. M. (2021). *Seas of the Russian Arctic in modern climatic conditions* (Saint-Petersburg: AARI), 360.

Bauch, D., Hölemann, J. A., Nikulina, A., Wegner, C., Janout, M. A., Timokhov, L. A., et al. (2013). Correlation of river water and local sea-ice melting on the Laptev Sea shelf (Siberian Arctic). *J. Geophys. Res. Oceans* 118, 550–561. doi: 10.1002/jgrc.20076

Bauch, D., Rutgers van der, L. M., Andersen, N., Torres-Valdes, S., Bakker, K., and Abrahamsen, E. P. (2011). Origin of freshwater and polynya water in the Arctic Ocean halocline in summer 2007. *Progr. Oceanogr.* 91, 482–495. doi: 10.1016/j.pocean.2011.07.017

Boyer, T. P., Baranova, O. K., Coleman, C., Garcia, H. E., Grodsky, A., Locarnini, R. A., et al. (2018). "World ocean database 2018," in *NOAA Atlas NESDIS 87*. Eds. S. Levitus and A. V. Mishonov (USA: Silver Spring).

Carmack, E., and Chapman, D. C. (2003). Wind-driven shelf/basin exchange on an Arctic shelf: The joint roles of ice cover extent and shelf-break bathymetry. *Geophys. Res. Lett.* 30, 1778. doi: 10.1029/2003GL017526

Carmack, E. C., Winsor, P., and Williams, W. (2015). The contiguous panarctic Riverine Coastal Domain: A unifying concept. *Progr. Oceanogr.* 139, 13–23. doi: 10.1016/j.pocean.2015.07.014

Carmack, E. C., Yamamoto–Kawai, M., Haine, T. W., Bacon, S., Bluhm, B. A., Lique, C., et al. (2016). Freshwater and its role in the Arctic Marine System: sources, disposition, storage, export, and physical and biogeochemical consequences in the

Arctic and global oceans. *J. Geophys. Res. Biogeosci.* 121, 675–717. doi: 10.1002/2015JG003140

Dawson, G., Landy, J., Tsamados, M., Komarov, A. S., Howell, S., Heorton, H., et al. (2022). A 10-year record of Arctic summer sea ice freeboard from CryoSat-2. *Rem. Sens. Environ.* 268, 112744. doi: 10.1016/j.rse.2021.112744

Demidov, A. B., Mosharov, S. A., and Makkaveev, P. N. (2014). Patterns of the Kara Sea primary production in autumn: Biotic and abiotic forcing of subsurface layer. *J. Mar. Sys.* 132, 130–149. doi: 10.1016/j.jmarsys.2014.01.014

Dewey, S. R., Morison, J. H., and Zhang, J. (2017). An edge-referenced surface fresh layer in the Beaufort Sea seasonal ice zone. *J. Phys. Oceanogr.* 47, 1125–1144. doi: 10.1175/JPO-D-16-0158.1

Dmitrenko, I., Kirillov, S., Eicken, H., and Markova, N. (2005). Wind-driven summer surface hydrography of the eastern Siberian shelf. *Geophys. Res. Lett.* 32, L14613. doi: 10.1029/2005GL023022

Duan, C., Dong, S., Xie, Z., and Wang, Z. (2019). Temporal variability and trends of sea ice in the Kara Sea and their relationship with atmospheric factors. *Polar Sci.* 20, 136–147. doi: 10.1016/j.polar.2019.03.002

Dubinina, E. O., Kossova, S. A., Miroshnikov, A. Y., and Kokryatskaya, N. M. (2017a). Isotope parameters (δD, δ18O) and sources of freshwater input to the Kara Sea. *Oceanology* 57, 31–40. doi: 10.1134/S0001437017010040

Dubinina, E. O., Kossova, S. A., Miroshnikov, A. Y., and Kokryatskaya, N. M. (2017b). Isotope (δD, δ18O) systematics in waters of the Russian Arctic seas. *Geochem. Int.* 55, 1022–1032. doi: 10.1134/S0016702917110052

Dubinina, E. O., Miroshnikov, A. Y., Kossova, S. A., and Shchuka, S. A. (2019). Modification of the Laptev Sea freshened shelf waters based on isotope and salinity relations. *Geochem. Int.* 57, 1–19. doi: 10.1134/S001670291901004X

Ekwurzel, B., Schlosser, P., Mortlock, R. A., and Fairbanks, R. G. (2001). River runoff, sea ice meltwater, and Pacific water distribution and mean residence times in the Arctic Ocean. *J. Geophys. Res. Oceans* 106, 9075–9092. doi: 10.1029/1999JC000024

Feng, D., Gleason, C. J., Lin, P., Yang, X., Pan, M., and Ishitsuka, Y. (2021). Recent changes to Arctic river discharge. *Nat. Commun.* 12, 6917. doi: 10.1038/s41467-021-27228-1

Fofonoff, N. P., and Millard, R. C. Jr. (1983). *Algorithms for the Computation of Fundamental Properties of Seawater* (UNESCO: Paris, France).

Golovin, P. N., and Ivanov, V. V. (2015). Density stratification effects on the ice lead heat balance and perennial ice melting in the Central Arctic. *Russ. Meteorol. Hydrol.* 40, 46–59. doi: 10.3103/S1068373915010070

Gordeev, V. V., Martin, J. M., Sidorov, J. S., and Sidorova, M. V. (1996). A reassessment of the Eurasian river input of water, sediment, major elements, and nutrients to the Arctic Ocean. *Am. J. Sci.* 296, 664–691. doi: 10.2475/ajs.296.6.664

Guay, C. K., and Falkner, K. K. (1998). Barium as a tracer of Arctic halocline and river waters. *Deep Sea Res. Pt II* 44, 1543–1569. doi: 10.1016/S0967-0645(97)00066-0

Haine, T. W., Curry, B., Gerdes, R., Hansen, E., Karcher, M., Lee, C., et al. (2015). Arctic freshwater export: Status, mechanisms, and prospects. *Glob. Planet. Change* 125, 13–35. doi: 10.1016/j.gloplacha.2014.11.013

Hall, S. B., Subrahmanyam, B., and Steele, M. (2023). The role of the Russian Shelf in seasonal and interannual variability of Arctic sea surface salinity and freshwater content. *J. Geophys. Res. Oceans* 128, e2022JC019247. doi: 10.1029/2022JC019247

Harms, I. H., and Karcher, M. J. (1999). Modeling the seasonal variability of circulation and hydrography in the Kara Sea. *J. Geophys. Res.* 104, 13431–13448. doi: 10.1029/1999JC900048

Janout, M. A., Holemann, J., Laukert, G., Smirnov, A., Krumpen, T., Bauch, D., et al. (2020). On the variability of stratification in the freshwater-influenced Laptev Sea region. *Front. Mar. Sci.* 7. doi: 10.3389/fmars.2020.543489

Jones, E. P., Anderson, L. G., Swift, J. H., Diego, S., and Jolla, L. (1998). Distribution of Atlantic and Pacific waters in the upper Arctic. *Geophys. Res. Lett.* 25, 765–768. doi: 10.1029/98GL00464

Kopylov, A. I., Zabotkina, E. A., Sazhin, A. F., Romanova, N., Belyaev, N., and Drozdova, A. (2023). Virioplankton and virus-induced mortality of prokaryotes in the Kara Sea (Arctic) in summer. *PeerJ* 11, e15457. doi: 10.7717/peerj.15457

Landy, J. C., Dawson, G., Tsamados, M., Bushuk, M., Stroeve, J. C., Howell, S. E. L., et al. (2022). A year-round satellite sea-ice thickness record from CryoSat-2. *Nature* 609, 517–522. doi: 10.1038/s41586-022-05058-5

Liang, H., and Su, J. (2021). Variability in sea ice melt onset in the Arctic northeast passage: Seesaw of the Laptev Sea and the East Siberian Sea. *J. Geophys. Res. Oceans* 126, e2020JC016985. doi: 10.1029/2020JC016985

Lin, P., Pickart, R. S., Vage, K., and Li, J. (2021). Fate of warm Pacific water in the Arctic basin. Geophys. *Res. Lett.* 48, e2021GL094693. doi: 10.1029/2021GL094693

MacKinnon, J. A., Simmons, H. L., Hargrove, J., Thomson, J., Peacock, T., Alford, M. H., et al. (2021). A warm jet in a cold ocean. *Nat. Commun.* 12, 2418. doi: 10.1038/s41467-021-22505-5

Makkaveev, P. N., Stunzhas, P. A., and Khlebopashev, P. V. (2010). The distinguishing of the Ob and Yenisei waters in the desalinated lenses of the Kara Sea in 1993 and 2007. *Oceanology* 50, 698–705. doi: 10.1134/S0001437010050073

Mosharov, S. A., Sazhin, A. F., Druzhkova, E. I., and Khlebopashev, P. V. (2018). Structure and productivity of the phytocenosis in the southwestern Kara Sea in early spring. *Oceanology* 58, 396–404. doi: 10.1134/S0001437018030141

Nummelin, A., Ilicak, M., Li, C., and Smedsrud, L. H. (2016). Consequences of future increased Arctic runoff on Arctic Ocean stratification, circulation, and sea ice cover. *J. Geophys. Res. Oceans* 121, 617–637. doi: 10.1002/2015JC011156

Osadchiev, A. A. (2021). Spreading and transformation of river discharge in the Russian Arctic. *Herald Russ. Acad. Sci.* 91, 694–699. doi: 10.1134/S1019331621060101

Osadchiev, A. A., Frey, D. I., Shchuka, S. A., Tilinina, N. D., Morozov, E. G., and Zavialov, P. O. (2021a). Structure of freshened surface layer in the Kara Sea during ice-free periods. *J. Geophys. Res. Oceans* 126, e2020JC016486. doi: 10.1029/2020JC016486

Osadchiev, A. A., Frey, D. I., Spivak, E. A., Shchuka, S. A., Tilinina, N. D., and Semiletov, I. P. (2021b). Structure and inter-annual variability of the freshened surface layer in the Laptev and East Siberian seas during ice-free periods. *Front. Mar. Sci.* 8. doi: 10.3389/fmars.2021.735011

Osadchiev, A. A., Medvedev, I. P., Shchuka, S. A., Kulikov, M. E., Spivak, E. A., Pisareva, M. N., et al. (2020b). Influence of estuarine tidal mixing on structure and spatial scales of large river plumes. *Ocean Sci.* 16, 1–18. doi: 10.5194/os-16-781-2020

Osadchiev, A. A., Pisareva, M. N., Spivak, E. A., Shchuka, S. A., and Semiletov, I. P. (2020a). Freshwater transport between the Kara, Laptev, and East Siberian seas. *Sci. Rep.* 10, 13041. doi: 10.1038/s41598-020-70096-w

Osadchiev, A., Sedakov, R., Frey, D., Gordey, A., Rogozhin, V., Zabudkina, Z., et al. (2023b). Intense zonal freshwater transport in the Eurasian Arctic during ice-covered season revealed by *in situ* measurements. *Sci. Rep.* 13, 16508. doi: 10.1038/s41598-023-43524-w

Osadchiev, A., Zabudkina, Z., Rogozhin, V., Frey, D., Gordey, A., Spivak, E. A., et al. (2023a). Structure of the Ob-Yenisei plume in the Kara Sea shortly before autumn ice formation. *Front. Mar. Sci.* 10. doi: 10.3389/fmars.2023.1129331

Paffrath, R., Laukert, G., Bauch, D., van der Loeff, M. R., and Pahnke, K. (2021). Separating individual contributions of major Siberian rivers in the Transpolar Drift of the Arctic Ocean. *Sci. Rep.* 11, 8216. doi: 10.1038/s41598-021-86948-y

Pavlov, V. K., and Pfirman, S. L. (1995). Hydrographic structure and variability of the Kara Sea: Implications for pollutant distribution. *Deep Sea Res. Pt II* 42, 1369–1390. doi: 10.1016/0967-0645(95)00046-1

Pipko, I. I., Pugach, S. P., and Semiletov, I. P. (2022). Dynamics of carbonate characteristics of the Kara Sea waters in the late autumn season 2021. *Dokl. Earth Sc.* 506, 671–676. doi: 10.1134/S1028334X22600232

Pogojeva, M., Zhdanov, I., Berezina, A., Lapenkov, A., Kosmach, D., Osadchiev, A., et al. (2021). Distribution of floating marine macro-litter in relation to oceanographic characteristics in the Russian Arctic Seas. *Mar. Pol. Bul.* 166, 112201. doi: 10.1016/j.marpolbul.2021.112201

Polyakov, I. V., Pnyushkov, A. V., Rember, R., Padman, L., Carmack, E. C., and Jackson, J. M. (2013). Winter convection transports Atlantic water heat to the surface layer in the eastern Arctic Ocean. *J. Phys. Oceanogr.* 43, 2142–2155. doi: 10.1175/JPO-D-12-0169.1

Randelhoff, A., and Sundfjord, A. (2018). Short commentary on marine productivity at Arctic shelf breaks: upwelling, advection and vertical mixing. *Ocean Sci.* 14, 293–300. doi: 10.5194/os-14-293-2018

Serreze, M. C., Barrett, A. P., Slater, A. G., Woodgate, R. A., Aagaard, K., Lammers, R. B., et al. (2006). The large-scale freshwater cycle of the Arctic. *J. Geophys. Res.* 111, C11010. doi: 10.1029/2005JC003424

Skyllingstad, E. D., Paulson, C. A., and Pegau, W. S. (2005). Simulation of turbulent exchange processes in summertime leads. *J. Geophys. Res.* 110, C05021. doi: 10.1029/2004JC002502

Spivak, E. A., Osadchiev, A. A., and Semiletov, I. P. (2021). Structure and variability of the Lena river plume in the south-eastern part of the Laptev Sea. *Oceanology* 61, 839–849. doi: 10.1134/S000143702106014X

Spreen, G., Kaleschke, L., and Heygster, G. (2008). Sea ice remote sensing using AMSR-E 89-GHz channels. *J. Geophys.Res.* 113, C02S03. doi: 10.1029/2005JC003384

Stroeve, J., and Notz, D. (2018). Changing state of Arctic sea ice across all seasons. *Env. Res. Lett.* 13, 103001. doi: 10.1088/1748-9326/aade56

Stunzhas, P. V. (1995). Separation of waters of the Yenisei and Ob rivers in the Kara Sea by alkalinity and silicon content. *Oceanology* 35, 215–219.

Sumata, H., de Steur, L., Divine, D. V., Granskog, M. A., and Gerland, S. (2023). Regime shift in Arctic Ocean sea ice thickness. *Nature* 615, 443–449. doi: 10.1038/s41586-022-05686-x

Supply, A., Boutin, J., Kolodziejczyk, N., Reverdin, G., Lique, C., Vergely, J.-L., et al. (2022). Meltwater lenses over the Chukchi and the Beaufort seas during summer 2019: From *in situ* to synoptic view. *J. Geophys. Res. Oceans* 127, e2021JC018388. doi: 10.1029/2021JC018388

Tank, S. E., McClelland, J. W., Spencer, R. G. M., Shiklomanov, A. I., Suslova, A., Moatar, F., et al. (2023). Recent trends in the chemistry of major northern rivers signal widespread Arctic change. *Nat. Geosci.* 16, 789–796. doi: 10.1038/s41561-023-01247-7

Timco, G. W., and Frederking, R. M. W. (1996). A review of sea ice density. *Cold Reg. Sci. Technol.* 24, 1–6. doi: 10.1016/0165-232X(95)00007-X

Timofeeva, A. B., and Sharatunova, M. V. (2021). Multiyear variability of the fast ice thickness in the Laptev Sea according to the polar station data. *Russian Arctic* 12, 62–76. doi: 10.24412/2658-4255-2021-1-62-76

Vihma, T. (2014). Effects of Arctic sea ice decline on weather and climate: A review. *Surv. Geophys.* 35, 1175–1214. doi: 10.1007/s10712-014-9284-0

Wassmann, P., Carmack, E. C., Bluhm, B. A., Duarte, C. M., Berge, J., Brown, K., et al. (2020). Towards a unifying pan-arctic perspective: A conceptual modelling toolkit. *Progr. Oceanogr.* 189, 102455. doi: 10.1016/j.pocean.2020.102455

Xie, L., Yakushev, E. V., Semiletov, I., Grinko, A., Gangnus, I., Berezina, A., et al. (2023). Biogeochemical structure of the Laptev Sea in 2015, 2017-2020 associated with the River Lena plume. *Front. Mar. Sci.* 10. doi: 10.3389/fmars.2023.1180054

Yakushev, E., Gebruk, A., Osadchiev, A., Pakhomova, S., Lusher, A., Berezina, A., et al. (2021). Microplastics distribution in the Eurasian Arctic is affected by Atlantic waters and Siberian rivers. *Commun. Earth Environ.* 2, 23. doi: 10.1038/s43247-021-00091-0

Yamamoto-Kawai, M., McLaughlin, F. A., Carmack, E. C., Nishino, S., and Shimada, K. (2008). Freshwater budget of the Canada Basin, Arctic Ocean, from salinity, δ18O, and nutrients. *J. Geophys. Res. Ocean* 113, 1–12. doi: 10.1029/2006JC003858

Zatsepin, A. G., Zavialov, P. O., Kremenetskiy, V. V., Poyarkov, S. G., and Soloviev, D. M. (2010). The upper desalinated layer in the Kara Sea. *Oceanology* 50, 657–667. doi: 10.1134/S0001437010050036

Zavialov, P. O., Izhitskiy, A. S., Osadchiev, A. A., Pelevin, V. V., and Grabovskiy, A. B. (2015). The structure of thermohaline and bio-optical fields in the upper layer of the Kara Sea in September 2011. *Oceanology* 55, 461–471. doi: 10.1134/S0001437015040177